framework upon dehydration/ rehydration processes, due to reversible movements of some organic moieties and hopping of some nickel atoms. The ability of MIL-77 inorganic network to accommodate glutarate derivatives was demonstrated by the use of 3-methylglutaric acid (3-MG) and 2-methylglutaric acid (2-MG). Moreover, we have shown that the handedness of the inorganic helices could be imposed by the configuration of the enantiopur 2-MG ligand. With cobalt ion, the synthesis of bulk homochiral solid has been confirmed by optical circular dichroism [2].

Here, we will summarize the structural features and the properties of this unique family of materials.

[1] Guillou N.; Livage C.; Drillon M; Férey G. ; *Angew. Chem. Int. Ed*, 2003, 42, 5314. [2] Livage C; Guillou N; Rabu P, Pattison P., Marrot J., Férey G. ; *Chemm. Commun.*, 2009, 30, **4**551.

Keywords: porous solids, chiral compounds, thermal transformation

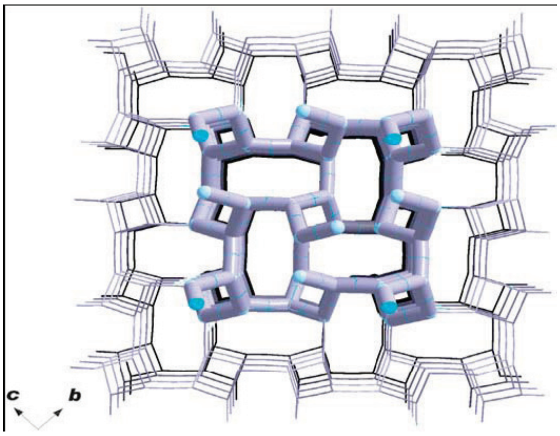

Fig. 1: View of the cubic (10, 3) chiral network

FA2-MS14-P16

Impact of pyroelectric $LiNbO_3$ and $LiTaO_3$ on water, organic dyes and *E. coli.*

Emanuel Gutmann[a], Annegret Benke[b], Katharina Gerth[b], Erik Mehner[a], Christin Klein[a], Udo Krause-Buchholz[c], Wolfgang Pompe[b], Dirk C. Meyer[a,d]. [a]*Institut für Strukturphysik, TU Dresden, Germany.* [b]*Institut für Werkstoffwissenschaft, TU Dresden, Germany.* [c]*Institut für Genetik, TU Dresden, Germany.* [d]*Institut für Experimentelle Physik, TU Bergakademie Freiberg, Germany.*
E-mail: emanuel.gutmann@physik.tu-dresden.de

$LiNbO_3$ and $LiTaO_3$ materials of polar crystal structure exhibit a spontaneous polarization that can be changed by temperature (pyroelectric effect). This leads to the generation of surface charges which are neutralized preferentially by external screening charges attracted from surrounding media [1]. In this context, we have investigated the impact of thermally excited pyroelectric $LiNbO_3$ and $LiTaO_3$ on the redox behavior of noble metal salts, and organic dyes in aqueous solutions. Based on various experimental results such as gold salt reduction, methylene blue degradation and conversion of dichlorofluorescin diacetate, a reaction mechanism including electron transfer and subsequent hydroxyl radical and hydrogen generation is proposed. Reaction rates strongly depend on the total surface of the pyroelectric particulate material in direct contact with the medium. As hydroxyl radicals are highly reactive oxidants used for disinfection purposes, also successful bactericidal tests with *Escherichia coli* have been performed.

[1] Yun Y., Kampschulte L., Li M., Liao D., Altman E.I., *J. Phys. Chem. C*, 2007, 111, 13951.

Keywords: polar crystal, pyroelectric effect, hydroxyl radical

FA2-MS14-P17

Synthesis of new stoichiometric barium bismuth borates $BaBi_2B_2O_7$, $BaBi_{10}B_6O_{25}$, $BaBi_8B_2O_{16}$.

Martun Hovhannisyan[a], Rafael Hovhannisyan[a], Hovakim Alexanyan[a], Nikolay Knyazyan[b]. [a]*Scientific-Production Enterprise of Material Science, Yerevan, Armenia.* [b]*Institute of General and Inorganic Chemistry of NAS RA, Yerevan, Armenia.*
E-mail: martun_h@yahoo.com

Interest to ternary alkali free bismuth borate systems M_xO_y-Bi_2O_3-B_2O_3 (M=Zn,Sr,Ca,Ba) studies has amplified recently. Various research groups worked in this area and revealed a number of ternary compounds, determined their structure, optical and nonlinear optical properties. Well known research groups payd special attention to BaO-Bi_2O_3-B_2O_3 system studies and have revealed four ternary stoichiometric $BaBiBO_4$ [1], $BaBiB_{11}O_{19}$, $BaBi_2B_4O_{10}$ and $Ba_3BiB_3O_9$[2,3] compounds in it.

Using methodology based on glass samples investigation was more effective at BaO-Bi_2O_3-B_2O_3 system phase diagram construction, than a traditional technique based on solid phase sintered samples studies. Because DTA curves of glasses, to the contrary DTA curves of solid state sintered samples, indicates their all characteristics temperatures, includes exothermal effects of glass crystallizations and endothermic effects of formed crystalline phases melting. Using different melts cooling rates we at first have determined large glass-forming field in the BaO-Bi_2O_3-B_2O_3 system, which includes all eutectics in the binary Bi_2O_3-B_2O_3, BaO-B_2O_3 and BaO-Bi_2O_3 systems and covers majority of the concentration triangles , reaching up to 90 mol% Bi_2O_3. BaB_4O_7, $Ba_2B_{10}O_{17}$, BaB_8O_{13}, $Bi_4B_2O_9$, $BiBO_3$, $Bi_3B_5O_{12}$, BiB_3O_6 and $Bi_2B_8O_{15}$ binary compounds formed stable glasses. BaB_2O_4, $Ba_2B_2O_5$ and $Bi_{24}B_2O_{39}$ compounds are in the area of glasses formed by high cooling rates (10^3-10^4)K/c.

Phase diagrams construction have allowed us to reveal three new $BaBi_2B_2O_7$ and $BaBi_{10}B_6O_{25}$ congruent melted at 725 and 690°C respectively and $BaBi_8B_2O_{16}$ incongruent melted at 725 compounds in the BaO-Bi_2O_3-B_2O_3 system through same compositions glass crystallization, because all ternary compounds have enough glass forming ability.

Single crystals of $BaBi_{10}B_6O_{25}$ were grown by cooling of a melt with the stoichiometric composition. Preliminary melted glass powder of the stoichiometric $11.11BaO\cdot 55.55Bi_2O_3\cdot 33.33B_2O_3$ (mol%) composition was heated in a uncovered quartz glass ampoule up to 750°C at a rate 10K/min. After 2h exposition at this temperature, the melt was cooled at a rate 0.5 K/h. Single crystals with size up to 1.66×0.38×0.19 mm^3 were grown.

The X-ray characteristics of new compounds were determined. X-ray powder diffraction patterns of $BaBi_2B_2O_7$ and $BaBi_{10}B_6O_{25}$ could be indexed on an orthorhombic cell with lattice parameters as follows: for $BaBi_2B_2O_7$ a=11.818Å, b=8.753 Å, c=7.146Å, cell volume V= 739.203 Å, Z=4; and

for $BaBi_{10}B_6O_{25}$ a= 6.434Å, b=11.763 Å, c=29.998 Å, cell volume V=2270.34 Å, Z=8.

[1] Barbier J., Penin N., Denoyer A., Cranswick L.M. *Solid State Sciences*, 2005, 7, 1055. [2] Egorysheva A.V., Kargin Yu.F *Zh.Neorg. Khim*. 2006, 7, 2078. [3] Egorysheva A.V., Skorikov V.M., Volodin V.D., Myslitskiy O.E. & Kargin Yu.F. *Zh.Neorg. Khim*. 2006, 12, 2078.

Keywords: $BaBi_2B_2O_7$, $BaBi_{10}B_6O_{25}$, $BaBi_8B_2O_{16}$

FA2-MS14-P18

Isomorphic (Mg, K) Substitution in Triple Molybdate $K_{3+x}Li_{1-x}Mg_4(MoO_4)_6$.

Tatyana Yu. Kardash[a], Zoya A. Solodovnikova[b], Sergey F. Solodovnikov[b], Evgeniya S. Zolotova[b]. [a]*Boreskov Institute of Catalysis, SB RAS, Novosibirsk, Russia.* [b]*Nikolaev Institute of Inorganic Chemistry, SB RAS, Novosibirsk, Russia.*
E-mail: kardash@catalysis.ru

Subsolidus phase relations in the ternary system Li_2MoO_4–K_2MoO_4–$MgMoO_4$ were studied at 480–570°C using X-ray powder diffraction (Bruker D8, CuKα), which revealed the existence of a new nonstoichiometric triple molybdate $K_{3+x}Li_{1-x}Mg_4(MoO_4)_6$ formed in the quasi binary join $K_2Mg_2(MoO_4)_3$–$Li_2Mg_2(MoO_4)_3$. The compound was found to be decomposed at 730°C into a solid mixture of β-$K_2Mg_2(MoO_4)_3$ and $Li_2Mg_2(MoO_4)_3$. The homogeneity range $0 \le x \le 0.25$ was found from the dependences of the trigonal unit cell parameters on the composition for powder samples quenched in air from 500°C (see Table). Crystals of the compound were obtained by spontaneous crystallization of the molten ceramic mixture $Li_2MoO_4 + 2K_2MoO_4 + 2MgMoO_4 + 2K_2Mo_2O_7$ cooled from 610°C. The crystal structure of $K_{3.11}Li_{0.89}Mg_4(MoO_4)_6$ (Bruker X8 Apex, a = 14.3541(2) Å, c = 19.7338(4) Å, sp. gr. $R\bar{3}c$, Z = 6, R = 0.0191) is isotypical to that of the sodium-ion conductor II-$Na_3Fe_2(AsO_4)_3$ = $(Na_5\square)^{IX}Na^{VI}Fe^{VI}Fe^{VI}{}_3(AsO_4)_6$ [1], and has the following cationic distribution: $(K_{0.5}\square_{0.5})_6(Mg_{0.89}K_{0.11})(Li_{0.89}Mg_{0.11})Mg_3(MoO_4)_6$. The main interatomic distances (Å) are: Mo–O 1.753(2)–1.768(2), K–O 2.771(2)–3.512(2), (Mg, K)–O 2.152(2) × 6, (Li, Mg)–O 2.075(2) × 6, Mg–O 2.034(2)–2.134(2). The structure comprises 3D framework built of MoO_4 tetrahedra and oxygen octahedra around three Mg-containing positions where each (Li, Mg)O_6 octahedron shares edges with three MgO_6 octahedra to form discrete octahedral tetra-clusters while the (Mg, K)O_6 octahedra are isolated. Large cavities of the framework are half occupied by K^+ ions. The unexpected feature of the structure is an isomorphic (Mg, K) substitution revealed for the first time. The analogous (Mn, K) and (Co, K) substitutions were early found in the isostructural compounds $K_{3.07}Li_{0.93}Mn_4(MoO_4)_6$ and $K_{3.30}Li_{0.70}Co_4(MoO_4)_6$ [2]. The open framework structures, the presence of defects in the $(K_{0.5}\square_{0.5})$ position and a structural relation of these three triple molybdates with the solid electrolyte II-$Na_3Fe_2(AsO_4)_3$ make us to suggest ionic exchange properties and an elevated ionic conductivity for the compounds considered.

Composition of sample	*a*, Å	*c*, Å
$K_{2.9}Li_{1.1}Mg_4(MoO_4)_6$*	14.350(1)	19.703(2)
$K_{3.0}Li_{1.0}Mg_4(MoO_4)_6$	14.350(1)	19.703(2)
$K_{3.1}Li_{0.9}Mg_4(MoO_4)_6$	14.353(1)	19.704(2)
$K_{3.2}Li_{0.8}Mg_4(MoO_4)_6$	14.358(1)	19.706(2)
$K_{3.3}Li_{0.7}Mg_4(MoO_4)_6$**	14.360(1)	19.709(2)

*$Li_2Mg_2(MoO_4)_3$ impurity. **β-$K_2Mg_2(MoO_4)_3$ impurity.

[1] D'Yvoire, F.; Bretey, E.; Collin G. *Solid State Ionics*, 1988, 28-30, 1259. [2] Solodovnikov, S.F.; Khaikina, E.G.; Solodovnikova, Z.A.; Kadyrova, Yu.M.; Khal'baeva, K.M.; Zolotova, E.S. *Doclady Chemistry*, 2007, 416, Part 1, 207.

Keywords: triple molybdate, nonstoichiometry, structure

FA2-MS14-P19

Nanostructured Random Type $MgFe_2O_4$ Spinel Prepared by Soft Mechanochemical Route.

A. Kremenovic[a,b], B. Antic[b], N. Jovic[b], M. Vucinic-Vasic[c]. [a]*University of Belgrade, Belgrade, Serbia.* [b]*The "Vinča" Institute, Belgrade, Serbia.* [c]*University of Novi Sad, Novi Sad, Serbia.*
E-mail: akremen@EUnet.rs

Results of structural, spectroscopic and magnetic investigations of $MgFe_2O_4$ nanoparticles prepared by soft mechanochemical synthesis will be reported. $MgFe_2O_4$ nanoparticles crystallize in $Fd\bar{3}m$ space group with mixed cation distribution and reduced percentage of Fe^{3+} at tetrahedral (8a) sites. Discrepancy in the cation distribution compared to that in the bulk Mg–ferrite is one of the highest known. X–ray line broadening analysis reveals crystallite size and strain anisotropy. The average apparent size is 10(1) nm and the average maximum strain is 27(2) x 10^{-4}. The projection of three-dimensional bodies representing "average apparent crystallite size" and "apparent maximum strain" on crystallographic (001) plane are given in Figure 1.

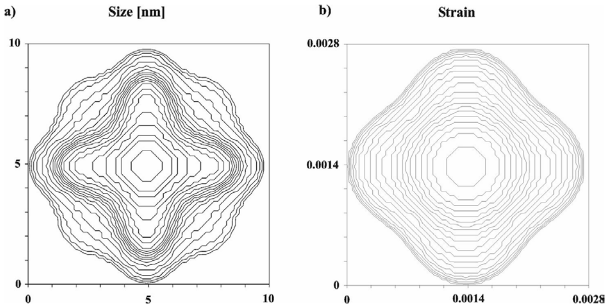

Figure 1. The projection of three-dimensional bodies representing (a) average apparent size and (b) maximum strain in crystallographic plane (001).

The saturation magnetization, M_{sat} = 62 emu/g measured at 5 K is twice higher than that found in the bulk counterparts. Such high value of M_{sat} is attributed to the low value of cation inversion parameter (δ=0.69), to the core/shell structure of the nanoparticles and to the surface/volume ratio. Mössbauer spectrum collected at room temperature reveals ferrimagnetic ordering between Fe^{3+} ions in 8*a* and 16*d* sites, while zero–field–cooled (ZFC) and field–cooled (FC) M(T) measurements were shown SPM state above 350 K.

Keywords: nanocrystals, microstructure analysis, magnetism